

See discussions, stats, and author profiles for this publication at: <https://www.researchgate.net/publication/260949173>

# 2013 Southeast Asian Smoke Haze: Fractionation of Particulate-Bound Elements and Associated Health Risk

ARTICLE in ENVIRONMENTAL SCIENCE & TECHNOLOGY · MARCH 2014

Impact Factor: 5.33 · DOI: 10.1021/es405533d · Source: PubMed

---

CITATIONS

20

---

READS

225

## 3 AUTHORS:



Raghu Betha

University of California, San Diego

20 PUBLICATIONS 173 CITATIONS

[SEE PROFILE](#)



Sailesh N. Behera

Shiv Nadar University

26 PUBLICATIONS 262 CITATIONS

[SEE PROFILE](#)



Rajasekhar Balasubramanian

National University of Singapore

235 PUBLICATIONS 3,347 CITATIONS

[SEE PROFILE](#)

## 2013 Southeast Asian Smoke Haze: Fractionation of Particulate-Bound Elements and Associated Health Risk

Raghu Betha,<sup>†,‡</sup> Sailesh N. Behera,<sup>†</sup> and Rajasekhar Balasubramanian<sup>†,‡,\*</sup>

<sup>†</sup>Department of Civil and Environmental Engineering, National University of Singapore (NUS), 1 Engineering Drive 2, E1A-07-03, 117576 Singapore

<sup>‡</sup>Singapore-MIT Alliance for Research and Technology (SMART), Centre for Environmental Sensing and Modeling (CENSAM), 1 CREATE Way, #10-01 CREATE Tower, 138602 Singapore

### Supporting Information

**ABSTRACT:** Recurring biomass burning-induced smoke haze is a serious regional air pollution problem in Southeast Asia (SEA). The June 2013 haze episode was one of the worst air pollution events in SEA. Size segregated particulate samples ( $2.5\text{--}1.0\ \mu\text{m}$ ;  $1.0\text{--}0.5\ \mu\text{m}$ ;  $0.5\text{--}0.2\ \mu\text{m}$ ; and  $<0.2\ \mu\text{m}$ ) were collected during the June 2013 haze episode.  $\text{PM}_{2.5}$  concentrations were elevated (up to  $329\ \mu\text{g}/\text{m}^3$ ) during the haze episode, compared to those during the nonhaze period ( $11\text{--}21\ \mu\text{g}/\text{m}^3$ ). Chemical fractionation of particulate-bound trace elements (B, Ca, K, Fe, Al, Ni, Zn, Mg, Se, Cu, Cr, As, Mn, Pb, Co, and Cd) was done using sequential extraction procedures. There was a 10-fold increase in the concentration of K, an inorganic tracer of biomass burning. A major fraction (>60%) of the elements was present in oxidizable and residual fractions while the bioavailable (exchangeable) fraction accounted for up to 20% for most of the elements except K and Mn. Deposition of inhaled potentially toxic trace elements in various regions of the human respiratory system was estimated using a Multiple-Path Particle Dosimetry model. The particle depositions in the respiratory system tend to be more severe during hazy days than those during nonhazy days. A prolonged exposure to finer particles can thus cause adverse health outcomes during hazy days. Health risk estimates revealed that the excessive lifetime carcinogenic risk to individuals exposed to biomass burning-impacted aerosols ( $18 \pm 1 \times 10^{-6}$ ) increased significantly ( $P < 0.05$ ) compared to those who exposed to urban air ( $12 \pm 2 \times 10^{-6}$ ).



### INTRODUCTION

Occurrence of biomass burning-induced smoke haze has become an annual phenomenon in tropical Southeast Asia (SEA) over the past several decades, but with different duration, intensity, and impacts, depending on prevailing weather conditions.<sup>1–11</sup> Uncontrolled forest and peat land fires resulting from land clearing activities in Indonesia release large amounts of airborne particulate matter (PM) with unique chemical composition into the atmosphere.<sup>4,5,12</sup> The resultant PM emissions from these wild fires are transported by trans-boundary winds and transformed into regional haze episodes affecting several countries in SEA, most notably, Singapore, Malaysia, Indonesia, and Thailand.<sup>1–11</sup> One of the worst haze episodes in the history of SEA occurred in June 2013.<sup>13</sup> An emergency was declared in Malaysia when the air pollution index (API) reached 746,<sup>14</sup> while an all-time high Pollution standard index (PSI) value of 401 (considered hazardous) was recorded in Singapore.

These smoke haze episodes are a growing threat to regional air quality and global climate change.<sup>15–17</sup> It was estimated that 13–40% (nearly, 0.81–2.57 Gt) of the mean annual global carbon emissions from fossil fuels were released into the atmosphere during the disastrous 1997 biomass burning haze

episode.<sup>18</sup> In addition to climatic and regional air quality impacts, the particulate pollution associated with biomass burning has severe impacts on human health.<sup>6,12</sup> Nearly a 30% increase in outpatient admission with an increase of 12% in upper respiratory tract illnesses, 19% in asthma, and 26% in rhinitis cases was recorded in Singapore during the 1997–1998 smoke haze.<sup>19</sup> A surge in hospital admissions related to respiratory illness was also reported during the 2013 haze episode.<sup>20</sup>

Several field studies were conducted to assess the potential environmental and health impacts of smoke haze through physicochemical characterization of PM.<sup>4–12</sup> In all previous studies, a major emphasis was placed on the characterization of  $\text{PM}_{2.5}$  (PM with aerodynamic diameter (AED)  $\leq 2.5\ \mu\text{m}$ ) in biomass burning induced smoke haze aerosols. However, submicrometer-sized particles ( $\text{PM}_1$  with AED  $\leq 1\ \mu\text{m}$ ) which comprise a significant fraction of  $\text{PM}_{2.5}$  have not been thoroughly investigated in terms of their chemical composition

**Received:** December 12, 2013

**Revised:** March 10, 2014

**Accepted:** March 19, 2014

**Published:** March 19, 2014



and health impacts. PM<sub>1</sub> can cause more adverse health impacts compared to coarse and fine particles.<sup>21,22</sup> These particles can easily penetrate deep into the respiratory system and are highly reactive due to the large surface area, leading to adverse health impacts. These submicrometer particles contain a complex mixture of organic and inorganic compounds such as carbonaceous material, PAHs, organic acids, metals, salts, and endotoxins.<sup>4,5</sup> The classification of health-relevant chemical components in these submicrometer particles is very important in understanding their potential health effects. However, to-date, no information regarding the chemical classification of biomass burning-impacted submicrometer particles in SEA is available in the literature. Among the various chemical components in PM, the fractionation of trace metals has particularly attracted a great deal of attention because of their potential health impacts.<sup>23–25</sup> Particulate-bound trace elements can induce acute and chronic effects on the lung when deposited in the lower respiratory tracts following environmental exposure.<sup>26</sup> Trace elements such as Cr, Ni, Cd, and Co are classified as carcinogenic, while other elements such as Al and Mn are toxic.<sup>27</sup> The exact mechanisms concerning the effect of trace elements on human health are not fully understood yet. However, recent evidence indicates that these bioavailable particulate-bound elements when deposited deep in the respiratory system undergo biochemical reactions, such as Fenton and Haber weiss reaction generating reactive oxygen species (ROS).<sup>28</sup> These ROS induce oxidative stress within cells, causing adverse health impacts.<sup>29</sup> It is, therefore, important to understand the specific form of particulate-bound trace elements since their bioavailability, solubility, and environmental transport largely depend on their chemical form.

In this study, we characterized the chemical fractionation of particulate-bound trace elements in size-segregated PM in smoke haze aerosols and background aerosols in Singapore during June–July and September–October 2013, respectively, for the first time. The specific forms of particulate-bound elements analyzed were (1) soluble and exchangeable metals; (2) carbonates, oxides, and reducible metals; (3) metals bound to organic matter, oxidizable and sulfidic metals; and (4) residual metals. The deposition of the particulate-bound elements in the respiratory system was estimated using a human airway deposition model (MPPD; Multiple Path Particle Dosimetry Model). In addition, carcinogenic and non-carcinogenic health risks were also evaluated due to the recurring smoke haze episodes in order to identify and implement suitable mitigation measures to protect the public health.

## MATERIALS AND METHODS

**Particulate Sampling.** Size-segregated PM samples (2.5–1.0  $\mu\text{m}$ , 1.0–0.5  $\mu\text{m}$ , 0.5–0.2  $\mu\text{m}$ , and <0.2  $\mu\text{m}$ ) were collected from 20 June 2013 through 28 July 2013 (haze period) and 12 September 2013 to 2 October 2013 (nonhaze period) using Dekati Gravimetric Impactor (DGI, Dekati ltd, Finland) at a tall building in the National University of Singapore (Supporting Information, SI, Figure S1). Ambient air was drawn through an impactor at a flow rate of 70 lpm for 12 h during hazy days ( $n = 6$ ) and for 24 h during normal days ( $n = 6$ ). The PM samples were collected onto 47 mm and 70 mm Teflon membrane (Polytetraflouoroethylene, PTFE) filter substrates. Further details of the sampling site and handling of filter and PM samples are provided in the SI.

**Sequential Extraction and Analysis.** A four step sequential extraction procedure was used to extract the different forms of trace metals from PM samples. The four different forms of trace metals extracted are as follows: (1) soluble and exchangeable metals (exchangeable fraction); (2) carbonates, oxides, and reducible metals (reducible fraction); (3) metals bound to organic matter, oxidizable and sulfidic metals (oxidizable fraction); and (4) residual metals. The details of the extraction procedure and the solvents used are provided in the SI (Table S1). Briefly, filters were microwave extracted using CH<sub>3</sub>COOH, NH<sub>2</sub>OH.HCl, H<sub>2</sub>O<sub>2</sub> + CH<sub>3</sub>COONH<sub>4</sub>, and HNO<sub>3</sub> + H<sub>2</sub>O<sub>2</sub> + HF sequentially for various metal fractions. The metal extracts were analyzed using an Inductive Coupled Plasma Mass Spectrometer (ICPMS) (ELAN 6100 PerkinElmer, Inc., MA, U.S.A.). Further details on quality control, analysis, and handling of filter extracts were provided in the SI.

**Estimation of Deposition Fraction.** We estimated the airway deposition of size fractionated aerosols by using the MPPD model.<sup>30</sup> Model adjustable assumptions of spherical particles with nose-only breathing, a tidal volume of 625 mL, and a breathing frequency of 12 breaths/min were made to simulate the respiratory system of an average human adult. Mass median aerodynamic diameter (MMAD) and geometric standard deviation (GSD) were estimated using log-probit method<sup>31</sup> to examine the difference in PM characteristics between hazy and nonhazy days and to use these values to estimate the deposition size fractions of PM mass using MPPD.

Size-resolved deposition fractions for each region of the respiratory tract (i.e., head, tracheobronchial, and pulmonary) were estimated using MPPD by selecting the option of multiple diameter (0.01–10  $\mu\text{m}$ ) as PM properties in the model. The deposition fraction curves were then separated for each size bin, representing four particle size fractions. The deposited mass of a chemical species in each size bin was estimated by multiplying the mass of a chemical species measured in a size bin by the corresponding size-resolved deposition fraction from MPPD results. The deposited masses found in each size bin were added to yield a combined PM<sub>2.5</sub> deposition. The specific deposition efficiency of each species was estimated in each respiratory tract as  $\mu\text{g}$  deposited per  $\mu\text{g}$  PM<sub>2.5</sub> mass inhaled during nonhaze and haze periods. The method used for estimation of specific efficiency of each chemical compound was adapted from the previous work by Ham et al.<sup>32</sup>

**Health Risk Assessment.** Human health risk was estimated in terms of excessive lifetime cancer risk (ELCR) and Hazard Quotient (HQ), based on the concentrations of elements determined through the experimental study. Health risk assessment is especially useful in understanding the health hazard associated with inhalation exposure to PM during the haze period. Elements such as Cd, Cr, Co, As, and Ni are classified as probable and possible carcinogenic compounds by International Agency for Research on Cancer (IARC).<sup>27</sup> Therefore, these compounds were used in estimation of cancer risk. The details and steps involved in health risk assessment are described in the SI.

**Backward Trajectory Analysis.** Backward air trajectory analysis is a useful tool to investigate the history of air masses. The latest, updated Hybrid Single-Particle Lagrangian Integrated Trajectory (HYSPPLIT) model,<sup>33</sup> developed by the National Oceanic and Atmospheric Administration (NOAA), was used to compute backward trajectories. Backward air trajectories were generated at eight starting times (every 3 h during each sampling event) for 48 h back in time with 100,

200, 500 m a.g.l. (above ground level). These atmospheric heights are very frequently used<sup>34</sup> and ensure that the trajectory starts in the atmospheric boundary layer (ABL).<sup>35</sup> In addition, backward trajectories at 1000 and 1500 m were generated near and above the atmospheric boundary layers, respectively. The error in a trajectory has been reported to be within 15–30% of the travel distance.<sup>33,36</sup>

## RESULTS AND DISCUSSION

**2013 Haze Episode.** The pollutant standards index (PSI), visibility, relative humidity (RH), and precipitation during hazy (20–28 June 2013) and nonhazy days (12 September–2 October 2013) are shown in Figure 1. On a clear normal day

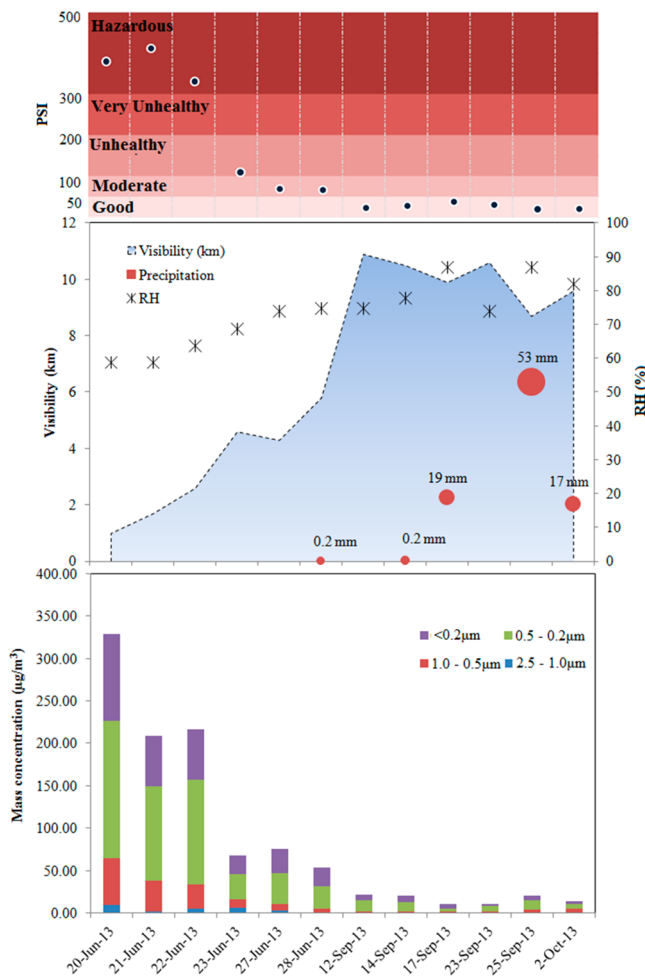


**Figure 1.** PSI, Visibility, Relative Humidity (RH), and particulate mass concentrations during the haze and nonhaze sampling period.

(PSI < 50; visibility: 8.7–10.9 km), moist weather conditions (RH: 75–87%) with occasional rain and thunder storms (precipitation: 0.2–53 mm) were observed. However, dry weather conditions (RH: 59–75%), with poor visibility (1–5.8 km) and very high PSI values (64–401) were observed during hazy days.

The most intense smoke haze episode (PSI: 401) that occurred on 21 June far exceeded the previous 1997 haze episodes (Highest PSI: 226) in terms of its severity, and is considered to be the worst smoke haze episode ever recorded in the history of Singapore.<sup>13,14</sup> Backward trajectories of air masses during the haze and non haze periods, constructed at

three different altitudes (a) above boundary layer (1500 m), (b) near boundary layer (1000 m), and (c) surface level (100 m), are shown in Figure 2. During the severe haze period (20–22 June 2013), air masses over the entire altitude range (surface to above boundary layer) transported smoke from the uncontrolled forest and peat fires (~200 to 500 km from the sampling location) to Singapore creating hazardous atmospheric conditions (PSI >300). However, on the remaining hazy days, the air masses near and above boundary layers only transported smoke emissions to Singapore. Air masses at the surface level that originated from the ocean and land masses were not significantly affected by wild fires. Additional trajectories generated at heights of 200 and 500 m were similar to those at 100 m. However, air trajectories began shifting toward the biomass burning sources only at 600 m and above, suggesting that smoke emissions from wild fires reached Singapore well above the surface levels and were intermixed with clean air masses transported into Singapore at the surface level by convective winds. Therefore, the severity of the smoke haze was relatively low during 23 – 28 June 2013. During the nonhaze periods, the air masses reaching Singapore originated from open Java and South China Sea at various altitudes. These air masses mainly comprised airborne particles emitted from ships, sea spray as well as local emissions within Singapore.

**Particulate Mass Concentrations.** Mass concentrations of particulate samples collected during hazy and nonhazy days are shown in Figure 1. The particles were categorized into 4 different size ranges 2.5–1.0  $\mu\text{m}$ , 1.0–0.5  $\mu\text{m}$ , 0.5–0.2  $\mu\text{m}$ , and <0.2  $\mu\text{m}$  (Quasi ultrafine particles; QUFPs). PM<sub>2.5</sub> concentrations (sum of mass concentrations of all 4 different size fractions) ranged from 54 to 329  $\mu\text{g}/\text{m}^3$  during the haze period, and were in the range of 11 – 21  $\mu\text{g}/\text{m}^3$  during non hazy days. Within the haze period, extremely high PM concentrations were observed from 20–22 June 2013 (209–329  $\mu\text{g}/\text{m}^3$ ) compared to other hazy days (54–69  $\mu\text{g}/\text{m}^3$ ). PM<sub>2.5</sub> measured during the haze period far exceeded the 24-h PM<sub>2.5</sub> guidelines recommended by the WHO (25  $\mu\text{g}/\text{m}^3$ ) and standards set by the USEPA (35  $\mu\text{g}/\text{m}^3$ ). The exceedance of the 24-h PM<sub>2.5</sub> standard is of particular health concern. The epidemiological study conducted by Pope et al.<sup>37</sup> reported that every 10  $\mu\text{g}/\text{m}^3$  increase in fine particles would increase the risk for death from lung cancer by 8%. Earlier studies on trans-boundary smoke haze in Singapore since 2000 have shown a two to 3-fold increase in PM<sub>2.5</sub> concentrations compared to nonhaze days.<sup>4,9</sup> However, in this study, the average PM<sub>2.5</sub> concentrations increased by 16 times during the severe haze period (20–22 June 2013) and 4 times on other hazy days; this increase is much higher when compared to earlier haze episodes. The particle size fractionation revealed that a major mass fraction of PM<sub>2.5</sub> consisted of particles in the size range of 0.5–0.2  $\mu\text{m}$  (haze: 43–57%; nonhaze: 39–60%), followed by quasi ultrafine particles (QUFPs < 0.2  $\mu\text{m}$  (haze: 27–42%; nonhaze: 25–41%). Particles in the size range of 1.0–0.5  $\mu\text{m}$  (haze: 8–17%; nonhaze: 8–15%) and 2.5–1.0  $\mu\text{m}$  (haze: 1–4%) made minor contributions to the total PM<sub>2.5</sub> concentrations. Among the different size fractions, the mass of the particles in the size range of 1.0–0.5  $\mu\text{m}$  increased sharply by a factor of 17 during the intense haze period (20–22 June 2013) followed by 0.5–0.2  $\mu\text{m}$  particles (a factor of 16), 2.5–1.0  $\mu\text{m}$  particles (a factor of 15) and QUFPs (<0.2  $\mu\text{m}$ ; a factor of 14). These results suggest that the mass of particles in all the size fractions increased during the smoke haze. However, the increase in

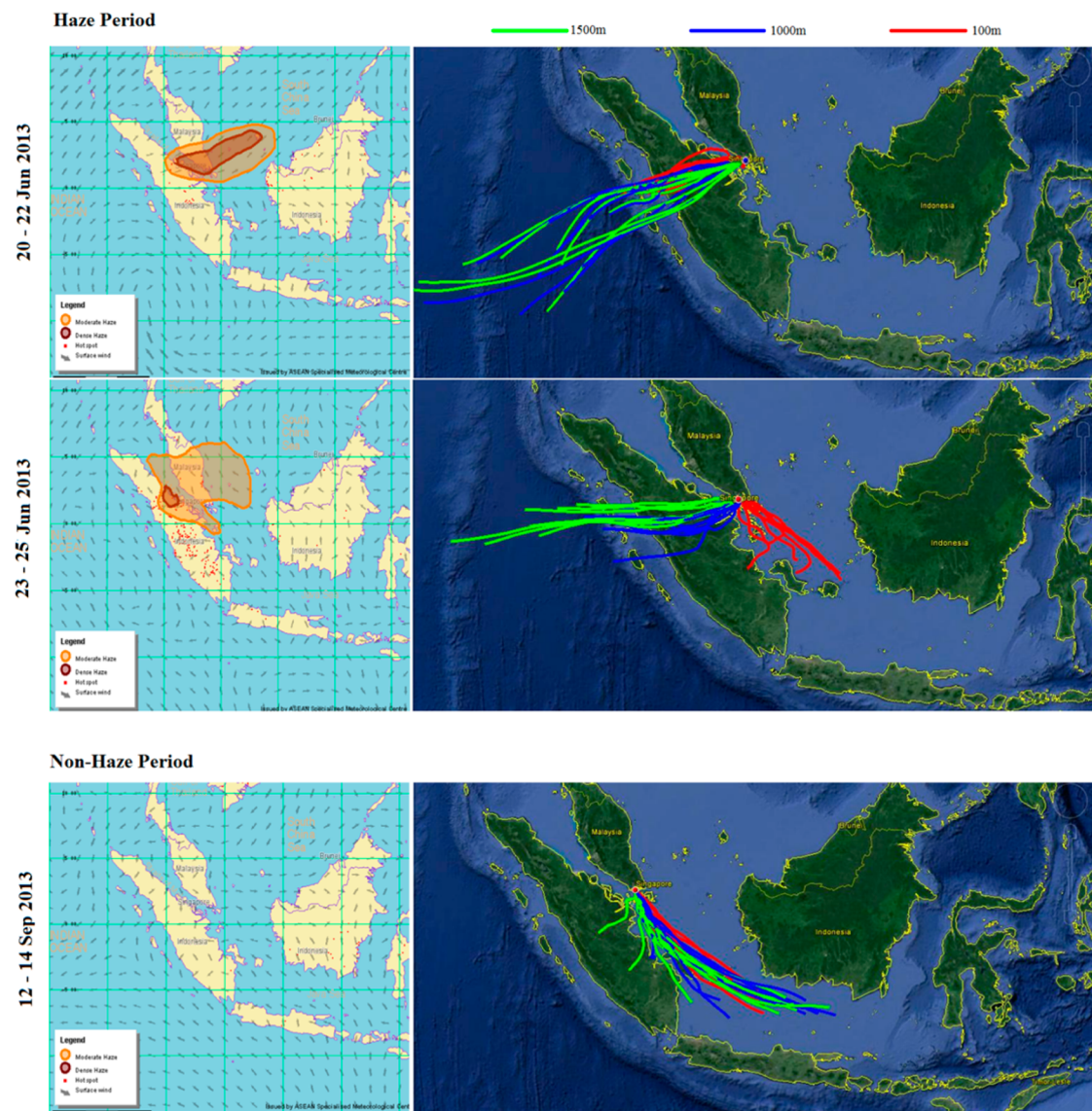


Figure 2. Backward air trajectories during haze (20–22 June 2013 and 23–25 Jun 2013) and nonhaze period (12–14 Sep 2013).

**Table 1. Mean Concentrations of Particulate Bound Elements in Various Particle Size Ranges during Haze and Non-Haze Periods**

(ng/m <sup>3</sup> )	haze				non-haze			
	2.5–1.0 μm	1.0–0.5 μm	0.5–0.2 μm	<0.2 μm	2.5–1.0 μm	1.0–0.5 μm	0.5–0.2 μm	<0.2 μm
B	2223.3 ± 953.2	2203.9 ± 864.4	2278.1 ± 731.4	2129.2 ± 636.4	555.0 ± 254.5	552.9 ± 243	551.8 ± 263.8	525.5 ± 255.5
Mg	35.3 ± 16.8	44.6 ± 20.5	29.3 ± 8.1	21.9 ± 4.5	9.1 ± 8.6	12.2 ± 4.6	9.1 ± 4.3	6.6 ± 3.3
Al	517.1 ± 190.9	544.5 ± 188.3	516.7 ± 150.1	468.7 ± 141.7	132.9 ± 73.9	130.7 ± 57.2	128.3 ± 62.9	123.2 ± 68.1
K	418.2 ± 135.8	484.3 ± 205.8	575.7 ± 155.5	592.4 ± 193.7	67.3 ± 59.4	53.6 ± 22.6	62.9 ± 34.4	83.3 ± 33.1
Ca	602.1 ± 182.6	636.9 ± 173.9	531.3 ± 103.2	459.9 ± 90.7	187.7 ± 126.8	174.7 ± 55.3	166.1 ± 71	166.2 ± 88.1
Cr	29.4 ± 12.5	29.9 ± 12.2	28.5 ± 9.0	29.0 ± 8.3	9.6 ± 7.4	7.5 ± 3.2	9.1 ± 6.7	8.6 ± 6.8
Mn	6.0 ± 2.3	7.6 ± 2.4	9.8 ± 7.2	7.8 ± 4.1	6.5 ± 11.6	1.9 ± 0.9	2.5 ± 1.0	2.9 ± 1.1
Fe	621.1 ± 398.7	574.8 ± 365.5	478.5 ± 194.8	388.3 ± 110.7	98.3 ± 67.9	89.1 ± 36.1	96.5 ± 51.0	90.5 ± 52.1
Co	1.8 ± 0.8	1.6 ± 0.5	1.6 ± 0.5	1.6 ± 0.3	0.9 ± 1	0.6 ± 0.6	0.6 ± 0.5	0.5 ± 0.4
Ni	99.6 ± 42.5	88.9 ± 38.4	89.8 ± 33.2	95.0 ± 25.3	49.7 ± 35.4	43.4 ± 27.5	41.6 ± 29.3	38.8 ± 27.1
Cu	29.4 ± 18.2	36.6 ± 31.6	27.9 ± 17.3	26.0 ± 11.6	12.8 ± 14.7	7.7 ± 5.7	7.7 ± 5.8	7.0 ± 4.7
Zn	81.0 ± 29.1	99.8 ± 40.3	96.8 ± 35.8	85.7 ± 13.4	23.0 ± 18.7	18.3 ± 7.1	25.3 ± 15.3	23.6 ± 15.9
As	28.5 ± 11.8	28.5 ± 12.9	27.4 ± 9.3	28.3 ± 7.9	9.0 ± 6.6	7.0 ± 3.2	7.3 ± 3.7	7.2 ± 3.5
Se	6.6 ± 1.5	8.1 ± 6.6	9.4 ± 1.8	9.1 ± 4.5	2.6 ± 1.9	2.6 ± 2.2	1.9 ± 1.3	2.0 ± 0.9
Cd	0.4 ± 0.1	0.3 ± 0.2	0.3 ± 0.2	0.3 ± 0.1	0.3 ± 0.4	0.1 ± 0.2	0.1 ± 0.1	0.1 ± 0.1
Pb	10.0 ± 4.3	10.0 ± 4.3	10.0 ± 3.3	9.6 ± 2.6	2.9 ± 1.6	2.4 ± 1.0	2.8 ± 1.5	2.7 ± 1.2

particle mass in the size range of 0.2–1.0  $\mu\text{m}$  in the atmosphere during the haze was relatively higher compared to QUFPs.

**Total Elemental Concentrations.** In this study, 16 particulate bound elements: K, B, Fe, Al, Ni, Zn, Mg, Ca, Cu, Cr, As, Mn, Pb, Co, Cd, and Se were analyzed. Mean concentrations of these elements are provided in Table 1 for various PM size ranges. The total concentration of elements analyzed constituted 13%, 10%, 8%, and 10% of PM<sub>2.5</sub>, PM<sub>1</sub>, PM<sub>0.5</sub>, and PM<sub>0.2</sub> mass, respectively during haze and 31%, 30%, 24%, and 27% during nonhaze periods. The percentage of particulate-bound elements is dependent on the amount of other chemical constituents present in PM, especially the carbonaceous matter. The smoke haze particles transported from peat and wild forest fires contain a large amount of organic and elemental carbon emitted due to biomass burning. The relative contributions of elements to the total mass of various PM fractions are therefore lower during the haze period when compared to the nonhaze period. Comparing atmospheric concentrations of individual elements (Table 1), it was observed that all the elements were increased by a factor of 3–12 during the haze period. Most of these elements are generated from various sources during biomass burning, which include peat smoldering, wood burning, incompletely combusted plants tissues, ash, and suspension of soil particles.<sup>38,39</sup> B, K, Fe, Al, and Ca were particularly found in higher concentrations compared to other elements for all size ranges of particles. K, an inorganic tracer for biomass burning, increased by a factor of 9–12, while the remaining elements showed an increase in the range of 3–7 with the exception of Fe (6–9) in different particle size fractions during the haze period, indicating a significant influence of smoke haze on the particulate-bound elemental concentrations. Enrichment factors (EF) for various elements were calculated to identify the elements of crustal and anthropogenic origin using the following equation, and the results are shown in SI Figure S2.

$$\text{EF}_x = (C_{xp}/C_{Alp})/(C_{xc}/C_{Aic}) \quad (3)$$

where EF<sub>x</sub> is the enrichment factor of an element x, C<sub>xp</sub> and C<sub>Alp</sub> are concentrations of an element x and Al, respectively, in PM, C<sub>xc</sub> and C<sub>Aic</sub> are their concentrations in average crustal materials.<sup>40</sup> EFs > 10 indicate a noncrustal source for the elements, while elements of crustal origin have EFs < 10. B, Ni, Zn, As, Se, Cu, Cr, As, Pb, Cd, and Co were found to be enriched in all the PM size fractions during both hazy and nonhazy days, indicating that noncrustal sources are the major contributors for these elements. However, Fe, Ca, Mn, K, and Mg have EFs < 10 for all PM size fractions during both haze and nonhaze days. Fe and Mn have EFs close to 1, suggesting that they are predominantly of crustal origin. However, K appears to be of mixed origin (crustal and noncrustal sources). As mentioned earlier, the primary sources of smoke haze in Indonesia are peat and agricultural land fires, suggesting that K could have been emitted from peat soil as well as biomass burning. Statistical *t* tests revealed that there is a significant difference ( $P < 0.05$ ) in the enrichment factors for K, Fe, Ni, Zn, and Cd between hazy and nonhazy days. However, the remaining elements have no significant difference ( $P > 0.05$ ).

**Classification of Elemental Concentrations in Various Particle Size Fractions.** Average concentrations of the different metal fractions: (i) exchangeable, (ii) reducible, (iii) oxidizable, and (iv) residual fractions, in various particle size ranges during hazy and nonhazy days are shown in SI Figure S3. B was found in very high concentrations during the haze

period compared to all the other elements, especially in the residual fraction. It was identified that nearly 8–20% of the global burden of atmospheric boron is attributable to coal, agricultural, fuel wood, and refuse burning.<sup>41</sup> Thus, the higher concentrations of B during the smoke haze episode can be attributed to agricultural and peat land fires. Crustal elements such as Al were also found in the residual fraction (haze: 88–91%; non-haze: 89–92%) while Ca (haze: 42–51%; non-haze: 39–45%) was mainly associated with organic matter. Fe was found to be mainly associated with organic matter in nonhaze samples (57–62%), while a major fraction of Fe in haze samples was found in the residual fraction (or silicate) (30–53%) for PM<sub>2.5–0.5</sub> and in the oxidizable fraction (46–51%) for PM<sub>0.5</sub>. K was found mostly in soluble and exchangeable fractions (31–53%). Cr (44–48%), Ni (47–53%), Cu (42–61%), Zn (56–66%), Pb (61–64%), and Se (21–41%) were found mainly in the oxidizable fraction, suggesting their association with organic matter. Carcinogenic elements such as Co were distributed equally between oxidizable and residual fractions for PM<sub>2.5–0.5</sub>, while a major fraction was found in the oxidizable fraction in PM<sub>0.5</sub>. Cd was distributed evenly among all the chemical fractions for PM<sub>0.2</sub>, while it was mainly found in the exchangeable fraction in PM<sub>0.2–1.0</sub>. A similar distribution of metals was observed for nonhaze samples as well with Co as an exception. Co existed in the oxidizable fraction predominantly for all size ranges in nonhaze samples.

Betha et al.<sup>12</sup> have reported similar results in their study on the chemical classification of PM<sub>2.5</sub> samples collected from peat fires in Indonesia. They also observed that nearly 90% of Al was in the residual fraction, significant amounts of Cr and Ni were found in the oxidizable fraction, Co was found significantly in both oxidizable and residual fractions, while Cd was found equally in exchangeable and oxidizable fractions. However, some variations in the fractions of metals exist between the previous study reported by Betha et al.<sup>12</sup> and this study. Betha et al.<sup>12</sup> observed a major fraction of Mn in reducible, and Pb, Cu, and Zn in residual fractions. However, in this study, a major fraction of Mn was found in the exchangeable fraction and that of Pb, Cu, and Zn in the oxidizable fraction. PM samples measured in this study were transported to Singapore by trans-boundary winds. These particles were “aged” with distance and time and chemically transformed through atmospheric photochemical reactions during their transport. In addition, several anthropogenic emissions during the course of their transport could have also influenced the chemical fractions.

Among the four chemical forms investigated in this study, the soluble and exchangeable fraction has high potential to cause adverse health effects since they can get readily dissolved and enter the bloodstream from lung fluids.<sup>42</sup> The remaining three fractions (reducible, oxidizable, and residual) are not very relevant in terms of health risk associated with inhalation of PM emissions. However, under certain pH conditions, the reducible fraction of metals may become bioavailable and pose a threat to human health.<sup>42</sup> These conditions could occur in acidic aerosols.<sup>43</sup> These bioavailable metals undergo biochemical reactions within cells and generate ROS causing cellular imbalance and oxidative stress on cells.<sup>28,29</sup> In addition, these particulate-bound metals could also be washed out by acidic rainfall and thus enter into water bodies through wet deposition, causing environmental and health-related problems. Oxidizable and residual fractions are not easily bioavailable, since these fractions of metals in airborne particulate matter are relatively stable.<sup>42</sup> Oxidizable and residual species together

contributed more than 60% of the total elemental concentrations. A major risk is therefore associated with the remaining 40% of the elements existing in exchangeable and reducible fractions. The exchangeable fraction of carcinogenic elements, such as Cr, Cd, Ni, Co, and As increased by a factor of 4, 4, 2, 5, and 6 during the haze period, suggesting that serious health risks are associated with inhalation of biomass burning-impacted particles. These elements were equally distributed among the various particle size fractions.

**Airway Deposition in the Respiratory System.** The average deposition fractions of PM<sub>2.5</sub>, PM<sub>1</sub>, PM<sub>0.5</sub>, and PM<sub>0.2</sub> in head, tracheobronchial, and pulmonary regions of the human respiratory system during the haze and nonhaze periods are shown in Figure 3. As described in a previous section, MMAD

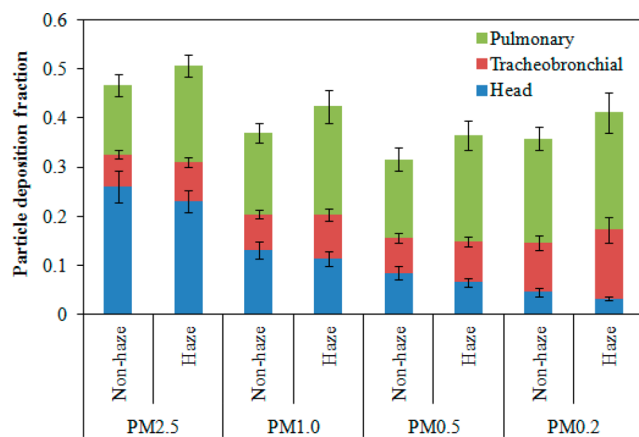


**Figure 3.** Deposition efficiencies of different particle fractions (PM<sub>2.5</sub>, PM<sub>1</sub>, PM<sub>0.5</sub>, PM<sub>0.2</sub>) in pulmonary, tracheobronchial, and head regions of the respiratory system during haze and nonhaze period.

and GSD were used in MPPD to estimate region specific deposition fractions. It should be noted that the average MMADs during hazy and nonhazy days were  $0.69 \pm 0.19 \mu\text{m}$  and  $0.58 \pm 0.16 \mu\text{m}$ , respectively, and similarly the corresponding average GSDs were  $2.6 \pm 0.6 \mu\text{m}$  and  $2.1 \pm 0.5 \mu\text{m}$ . The deposition of larger fractions of PM<sub>2.5</sub> on the head airways was due to a combination of sedimentation, and the impaction of particles onto the larynx and airway bifurcations.<sup>44</sup> The reason for more deposition of submicrometer particles in the pulmonary region was due to the flow path of smaller particles in the human respiratory system, which is primarily governed by Brownian diffusion leading to preferential deposition in the pulmonary region.<sup>32,45</sup> Overall, it has been observed that the particle depositions in the respiratory system would be more severe during the haze period than those during nonhaze periods. A possible reason is that haze events produce larger particles, which shift the median aerosol size to the right on the deposition curve leading to a higher total deposition. A similar observation was reported by Lai et al.,<sup>46</sup> in which it was found that large particles were formed during haze episodes, caused by transport of emissions from rice straw burning. The mass median diameters were  $0.92$  and  $1.21 \mu\text{m}$  during non-burning and burning periods, respectively. It is also evident that during the long-range transport of biomass emissions, some finer particles agglomerated, resulting in an increase in sizes of particles, as well during haze events.<sup>4,12</sup> The statistical analysis showed that the *p*-values were less than 0.05 for hazy days versus nonhazy days for deposition fractions at all regions of the respiratory system and indicated that the results were

significantly different with a 95% confidence limit. More interestingly, the average deposition fractions of PM<sub>2.5</sub>, PM<sub>1</sub>, PM<sub>0.5</sub>, and PM<sub>0.2</sub> in tracheobronchial and pulmonary regions increased, while they decreased in the head airway region during the haze period, which can be attributed to enrichment of submicrometer particles in the accumulation mode during the haze period. The average deposition efficiencies of all elements of PM<sub>2.5</sub> in head, tracheobronchial, and pulmonary regions of the respiratory system during the haze and nonhaze periods were estimated using the MPPD model, and are shown in SI Figure S4. These deposition efficiencies were later used in the calculation of health risk assessment. The particle size of PM<sub>2.5</sub> was only considered since it is commonly regulated as part of ambient air quality standards. The total deposition efficiency (the sum of head, tracheobronchial, and pulmonary regions) varied from 33% (Mg) to 51% (Ca) and 40% (Mg) to 56% (Ca) during nonhaze and haze periods, respectively. For deposition in the head region, Cr had the lowest amount with 14% and 13% during nonhaze and haze periods, respectively. The highest deposition in the head region was observed by Ca as 28% and 23% during the nonhaze period and haze periods, respectively. Similar to the observations on the deposition in the pulmonary region, trace elements also exhibited the trends of more deposition in the tracheobronchial region during the haze period, compared to those during the non-haze period. The statistical analysis confirmed that the deposition efficiencies were significantly different ( $P < 0.05$ ) during hazy days from those during nonhazy days for all elements (except Al, Fe, and Cu) in all regions of the respiratory system.

**Health Risk Assessment.** Smoke haze episodes occur almost every year in SEA, causing a serious concern for regional air quality and public health. Human health risk assessment for inhalation of ambient PM<sub>2.5</sub> was therefore carried out, as described in the Material and Methods. Health risk assessment was conducted for two possible scenarios to assess the impact of recurring smoke haze on public health. In the first scenario, it was assumed that there are no fire events, i.e., no smoke haze episodes in the region and thus the health risk estimates (HRE<sub>I</sub>: health risk estimates for scenario I) reflect the exposure to local anthropogenic and natural emissions during the lifetime of individuals. In the second scenario, biomass burning and recurring smoke haze episodes along with local anthropogenic sources were considered in estimating health risk (HRE<sub>II</sub>: health risk estimates for Scenario II). Since the particles deposited in upper (head) and intermediate (trachea bronchial) levels of the respiratory system are excreted out easily by the natural defense mechanisms of the respiratory system, we considered only the deposition efficiencies of particulate-bound metals in the pulmonary region (estimated through the airway MPPD model) for calculation of health risk.

To estimate HRE<sub>I</sub>, exposure concentrations were calculated for the entire lifetime (70 yrs) assuming that a person is exposed throughout the year to the ambient concentrations of particulate-bound elements measured during nonhaze periods, as considered in this study. For HRE<sub>II</sub>, it was assumed that recurring smoke haze episodes occur for 10 days in a year, and therefore, the person is exposed to ambient concentrations of particulate-bound elements in PM<sub>2.5</sub> measured during those hazy days in a year and to the ambient concentrations measured during nonhaze days in the remaining 355 days of the year. The soluble and exchangeable fraction of the total metal concentrations was only used in calculations since they are bioavailable and impose adverse health impacts.

Sample calculations of health risk estimates for the two exposure scenarios are shown in SI Table S2. As a conservative approach, we assumed ET as 8 h/day. The results indicated that HQ is below the acceptable limit of 1. However, ELCR exceeded the acceptable limit ( $1 \times 10^{-6}$ ) for both scenarios. It was observed that ELCR for HRE<sub>I</sub> was  $12 \pm 2 \times 10^{-6}$ , implying that 10 to 14 individuals in a million are likely to develop cancer in a lifetime due to the exposure to local anthropogenic PM<sub>2.5</sub> emissions. However, when smoke haze episodes due to biomass and peat burning are considered in health risk estimates (HRE<sub>II</sub>), ELCR increased significantly ( $P < 0.05$ ) by nearly 50% to  $18 \pm 1 \times 10^{-6}$  indicating a considerable impact of biomass smoke haze episodes on public health. Though the smoke haze episodes occur for a short duration (10 days/year), their repeated occurrence every year is likely to pose adverse long-term impacts on public health. In addition, peat fires are prone to be more intense, widespread, and frequent during El Niño years than those in other years, which could further increase the public health risk. An El Niño/Southern Oscillation (ENSO) phenomenon significantly reduces the amount of rainfall and prolongs dry spells in SEA, resulting in a longer duration of smoke haze episodes with high concentrations of PM. It was reported that the frequency of El Niño years is likely to increase in the future.<sup>47</sup> It should be noted that the soluble concentrations of elements such as Cr, Ni are not entirely carcinogenic; only Cr(VI) and certain forms of nickel and nickel compounds are carcinogenic. In addition, the soluble concentration of these metal forms in the lung fluid would give realistic data for calculation of health risk estimates. However, in this study, we did not measure the concentrations of specific chemical forms, nor did we use the lung fluid to estimate soluble concentrations. Therefore, the data used in risk calculations may result in slight overestimation of the health risk. In this study, organic compounds, such as PAHs were not used in calculating health risk estimates. These organic compounds, the product of incomplete combustion, are likely to be found in significant quantities in smoke haze aerosols and thus pose severe health risks.

The recurring smoke haze episodes in the SEA region due to peat and forest fires in Indonesia have severe implications on regional air quality and public health. The haze episode in 2013 was undoubtedly the worst haze episode in SEA in the past two decades. Atmospheric PM<sub>2.5</sub> concentrations reached as high as  $329 \mu\text{g}/\text{m}^3$  (~13 times that of WHO safe limits). The smoke haze episodes were intense during 20–22 June 2013 since the particle air masses reaching Singapore from the surface to above the boundary layer directly originated from the main cluster of peat and forest fires in Sumatra. As a result of a shift in surface winds after 22 Jun 2013, the intensity of trans-boundary smoke haze was slightly reduced. Most of the PM mass was found in submicrometer particle size ranges (>90%), and the atmospheric loading of these submicrometer particles increased significantly during the haze period. As a consequence, the particle deposition efficiencies in lower respiratory system increased for submicrometer particles during the haze period. Increased concentrations of particulate-bound toxic and carcinogenic elements in the atmosphere were observed during the smoke haze. A major fraction of the elemental concentration was either bound to organic matter or found in the residual fraction bound to silicate for most of the elements. Although the bioavailable fraction was a minor component, health risk estimates indicate a significant impact of these elements on human health. Human exposure to smoke haze

episodes occurred for a shorter duration of time (i.e., 10 days a year). However, their annual recurrence in the region could increase the health risk for the public by nearly 50%. This study thus reveals that airborne particles arising from recurring biomass and peat fires in SEA are quite detrimental to public health. Proactive measures should therefore be undertaken to curb the occurrence of trans-boundary biomass smoke haze episodes with the use of remote sensing methods to provide local authorities in Indonesia with high resolution satellite images of hot spots and to implement effective environmental policy regulations.

## ASSOCIATED CONTENT

### **S Supporting Information**

Experimental protocol for sequential extraction of particulate bound elements; crustal enrichment factors of various elements; concentrations of individual elements in various fractions (exchangeable, reducible, oxidizable, and residual metals) during haze and nonhaze periods for various size ranges; specific deposition efficiencies of various elements bound to PM<sub>2.5</sub> in pulmonary, tracheobronchial, and head regions during haze and nonhaze periods; description of health risk assessment; description of sampling site; handling; quality control, analysis, and handling of filter extracts. This material is available free of charge via the Internet at <http://pubs.acs.org>.

## AUTHOR INFORMATION

### Corresponding Author

\*Tel: +65- 65165135; fax: +65-67744202; e-mail: ceerbala@nus.edu.sg.

### Notes

The authors declare no competing financial interest.

## ACKNOWLEDGMENTS

This work was financially supported by the National University of Singapore (Grant No: R-302-000-082-133) and Singapore-MIT Alliance for Research and Technology's CENSAM research programme (Grant: R-302-000-076-592). Betha, R., thanks CENSAM for supporting his post doctoral studies at NUS.

## REFERENCES

- (1) Nichol, J. Smoke haze in Southeast Asia: A predictable reoccurrence. *Atmos. Environ.* **1998**, *32* (14/15), 2715–2716.
- (2) Radojevic, M. Chemistry of forest fires and regional haze with emphasis on Southeast Asia. *Pure. Appl. Geophys.* **2003**, *160* (1–2), 157–187.
- (3) Heil, A.; Goldammer, J. G. Smoke-haze pollution: A review of the 1997 episode in Southeast Asia. *Reg. Environ. Change* **2001**, *2* (1), 24–37.
- (4) See, S. W.; Balasubramanian, R.; Wang, W. A study of the physical, chemical, and optical properties of ambient aerosol particles in Southeast Asia during hazy and nonhazy days. *J. Geophys. Res.* **2006**, *111* (D10), D10S08 <http://dx.doi.org/10.1029/2005JD006180>.
- (5) See, S. W.; Balasubramanian, R.; Rianawati, E.; Karthikeyan, S.; Streets, D. G. Characterization and source apportionment of particulate matter  $\leq 2.5 \mu\text{m}$  in Sumatra, Indonesia during a recent peat fire episode. *Environ. Sci. Technol.* **2007**, *41* (10), 3488–3494.
- (6) Pavagadhi, S.; Betha, R.; Venkatesan, S.; Balasubramanian, R.; Hande, M. P. Physicochemical and toxicological characteristics of urban aerosols during a recent Indonesian biomass burning episode. *Environ. Sci. Poll. Res.* **2013**, *20* (4), 2569–2578.
- (7) Atwood, S. A.; Reid, J. S.; Kreidenweis, S. M.; Yu, L. E.; Salinas, S. V.; Chew, B. N.; Balasubramanian, R. Analysis of source regions for

- smoke events in Singapore for the 2009 El Nino burning season. *Atmos. Environ.* **2013**, *78*, 219–230.
- (8) Reid, J. S.; Hyer, E. J.; Johnson, R. S.; Holben, B. N.; Yokelson, R. J.; Zhang, J.; Campbell, J. R.; Chritopher, S. A.; Giroldo, L. D.; Giglio, L.; Holz, R. E.; Kearney, C.; Miettinen, J.; Reid, E. A.; Turk, J.; Wang, J.; Xian, P.; Zhao, G.; Balasubramanian, R.; Chew, B. N.; Janjal, S.; Lagrosas, N.; Lestari, P.; Lin, N.-H.; Mahmud, M.; Nguyen, A. X.; Norris, B.; Oanh, N. T. K.; Oo, M.; Salinas, V.; Welton, E. J.; Liew, S. C. Observing and understanding the Southeast Asian aerosol system by remote sensing: An initial review and analysis for the Seven Southeast Asian Studies (7SEAS) program. *Atmos. Res.* **2013**, *122*, 403–468.
- (9) Salinas, S. V.; Chew, B. N.; Miettinen, J.; Campbell, J. R.; Welton, E. J.; Reid, J. S.; Yu, L. E.; Liew, S. C. Physical and optical characteristics of the October 2010 haze event over Singapore: A photometric and lidar analysis. *Atmos. Res.* **2013**, *122*, 555–570.
- (10) Huang, K.; Fu, J. S.; Hsu, N. C.; Gao, Y.; Dong, X.; Tsay, S.-C.; Lam, Y. F. Impact assessment of biomass burning on air quality in Southeast and East Asia during BASE-ASIA. *Atmos. Environ.* **2013**, *78*, 291–302.
- (11) Lin, N. H.; Tsay, S.-C.; Maring, H. B.; Yen, M.-C.; Sheu, G.-R.; Wang, S.-H.; Chi, K. H.; Chuang, M.-T.; Ou-Yang, C.-F.; Fu, J. S.; Reid, J. S.; Lee, C.-T.; Wang, L.-C.; Wang, J.-L.; Hsu, C. N.; Sayer, A. M.; Holben, B. N.; Chu, Y.-C.; Nguyen, X. A.; Sopajaree, K.; Chen, S.-J.; Cheng, M.-T.; Tsuang, B.-J.; Tsai, C.-J.; Peng, C.-M.; Schnell, R. C.; Conway, T.; Chang, C.-T.; Lin, K.-S.; Tsai, Y. I.; Lee, W.-J.; Chang, S.-C.; Liu, J.-J.; Chiang, W.-L.; Huang, S.-J.; Lin, T.-H.; Liu, G.-R. An overview of regional experiments on biomass burning aerosols and related pollutants in Southeast Asia: From BASE-ASIA and the Dongsha Experiment to 7-SEAS. *Atmos. Environ.* **2013**, *78*, 1–19.
- (12) Betha, R.; Pradani, M.; Lestari, P.; Joshi, U. M.; Reid, J. S.; Balasubramanian, R. Chemical speciation of trace metals emitted from Indonesian peat fires for health risk assessment. *Atmos. Res.* **2013**, *122*, 571–578.
- (13) Singapore haze hits record high from Indonesia fires. BBC News Asia. 21 June 2013, <http://www.bbc.co.uk/news/world-asia-22998592> (Accessed: 9 December 2013).
- (14) Malaysia declares state of emergency in Muar and Ledang. New Straits Times. 23 June 2013, <http://news.asiaone.com/News/Haze/Story/A1Story20130623-431746.html> (Accessed: 9 December 2013).
- (15) Page, S. E.; Rieley, J. O.; Banks, C. J. Global and regional importance of the tropical peatland carbon pool. *Global Change Biol.* **2011**, *17* (2), 798–818.
- (16) Tosca, M. G.; Randerson, J. T.; Zender, C. S.; Flanner, M. G.; Rasch, P. J. Do biomass burning aerosols intensify drought in equatorial Asia during El Niño? *Atmos. Chem. Phys.* **2010**, *10* (8), 3515–3528.
- (17) Koe, L. C. C.; Arellano, A. F.; McGregor, J. L. Investigating the haze transport from 1997 biomass burning in Southeast Asia: Its impact upon Singapore. *Atmos. Environ.* **2001**, *35*, 2723–2734.
- (18) Page, S. E.; Siegert, F.; Rieley, J. O.; Boehm, H. D. V.; Jaya, A.; Limin, S. The amount of carbon released from peat and forest fires in Indonesia during 1997. *Nature* **2002**, *420*, 61–65.
- (19) Emmanuel, S. C. Impact to lung health of haze from forest fires: the Singapore experience. *Respirology* **2000**, *5* (2), 175–182.
- (20) Haze update: Hospitals seeing more patients with breathing problems, asthma. The Straits Times. 20 June 2013, <http://www.straitstimes.com/the-big-story/the-haze-singapore/story/haze-update-hospitals-seeing-more-patients-breathing-problems> (Accessed: 21st November 2013).
- (21) Russell, A. G.; Brunekreef, B. A focus on particulate matter and health. *Environ. Sci. Technol.* **2009**, *43* (13), 4620–4625.
- (22) Farina, F.; Sancini, G.; Longhin, E.; Mantecca, P.; Camatini, M.; Palestini, P. Milan PM1 induces adverse effects on mice lungs and cardiovascular system. *BioMed. Res. Int.* **2013**, Article ID: 583513.
- (23) Mbengue, S.; Alleman, L. Y.; Flament, P. Size-distributed metallic elements in submicronic and ultrafine atmospheric particles from urban and industrial areas in northern France. *Atmos. Res.* **2014**, *135*–136, 35–47.
- (24) Richter, P.; Grino, P.; Ahumada, I.; Giordano, A. Total element concentration and chemical fractionation in airborne particulate matter from Santiago, Chile. *Atmos. Environ.* **2007**, *41*, 6729–6738.
- (25) Betha, R.; Balasubramanian, R. Emissions of particulate-bound elements from biodiesel and ultra low sulfur diesel: Size distribution and risk assessment. *Chemosphere* **2013**, *90*, 1005–1015.
- (26) Bradshaw, L. M.; Fishwick, D.; Slater, T.; Pearce, N. Chronic bronchitis, work related respiratory symptoms, and pulmonary function in welders in New Zealand. *Occup. Environ. Med.* **1998**, *55* (3), 150–154.
- (27) IARC. Agents classified by the IARC Monographs, **2013**, Vol: 1–108. Website accessed on 4 Sep 2013.
- (28) Li, N.; Hao, M. Q.; Phalen, R. F.; Hinds, W. C.; Nel, A. E. Particulate air pollutants and asthma. A paradigm for the role of oxidative stress in PM-induced adverse health effects. *Clin. Immunol.* **2003**, *109* (3), 250–265.
- (29) Halliwell, B. Reactive oxygen species in living systems e source, biochemistry, and role in human-disease. *Am. J. Med.* **1991**, *91* (3C), S14–S22.
- (30) Asgharian, B.; Anjilvel, S. A Multiple-path model of fiber deposition in the rat lung. *Toxicol. Sci.* **1998**, *44* (1), 80–86.
- (31) O'Shaughnessy, P. T.; Raabe, O. G. A Comparison of Cascade Impactor Data Reduction Methods. *Aerosol. Sci. Technol.* **2003**, *37* (2), 187–200.
- (32) Ham, W. A.; Ruehl, C. R.; Kleeman, M. J. Seasonal variation of airborne particle deposition efficiency in the human respiratory system. *Aerosol. Sci. Technol.* **2011**, *45* (7), 795–804.
- (33) Draxler, R. R.; Hess, G. D. Description of the HYSPLIT 4 Modeling System. NOAA Technical Memorandum. 2004, ERL ARL-224.
- (34) Erel, Y.; Kalderon-Asael, B.; Dayan, U.; Sandler, A. European atmospheric pollution imported by cooler air masses to the Eastern Mediterranean during the summer. *Environ. Sci. Technol.* **2007**, *41* (15), 5198–5203.
- (35) Dvorská, A.; Lammel, G.; Holoubek, I. Recent trends of persistent organic pollutants in air in central Europe-Air monitoring in combination with air mass trajectory statistics as a tool to study the effectiveness of regional chemical policy. *Atmos. Environ.* **2009**, *43*, 1280–1287.
- (36) Stohl, A. Computation, accuracy and application of trajectories—A review and bibliography. *Atmos. Environ.* **1998**, *32*, 947–966.
- (37) Pope, C. A., III; Hill, R. W.; Villegas, G. M. Particulate air pollution and daily mortality on Utah's Wasatch Front. *Environ. Health. Perspect.* **1999**, *107* (7), 567–573.
- (38) Gaudichet, A.; Echalar, F.; Chatenet, B.; Quisefit, J. P.; Malingre, G.; Cachier, H.; Buatmenard, P.; Artaxo, P.; Maenhaut, W. Trace-elements In tropical African savanna biomass burning aerosols. *J. Atmos. Chem.* **1995**, *22* (1–2), 19–39.
- (39) Karthikeyan, S.; Balasubramanian, R.; Iouri, K. Particulate air pollution from bushfires: human exposure and possible health effects. *J. Toxicol. Environ. Health A* **2006**, *69* (21), 1895–1908.
- (40) Balasubramanian, R.; Qian, W.-B. Characterization and source identification of airborne trace metals in Singapore. *J. Environ. Monit.* **2004**, *6* (10), 813–818.
- (41) Anderson, D. L.; Kitto, M. E.; McCarthy, L.; Zoller, W. H. Sources and atmospheric distribution of particulate and gas-phase Boron. *Atmos. Environ.* **1994**, *28*, 1401–1410.
- (42) Espinosa, A. J. F.; Rodriguez, M. T.; Rosa, J. B.; Sánchez, J. C. J. A chemical speciation of trace metals for fine urban particles. *Atmos. Environ.* **2002**, *36*, 773–780.
- (43) Behera, S. N.; Betha, R.; Liu, P.; Balasubramanian, R. A study of diurnal variations of PM<sub>2.5</sub> acidity and related chemical species using a new thermodynamic equilibrium model. *Sci. Total Environ.* **2013**, *452*–453, 286–295.
- (44) Zhang, L.; Yu, C. P. Empirical equations for nasal deposition of inhaled particles in small laboratory—Animals and humans. *Aerosol. Sci. Technol.* **1993**, *19* (1), 51–56.

- (45) Ingham, D. B. Diffusion of aerosols from a stream flowing through a short cylindrical pipe. *J. Aerosol. Sci.* **1984**, *15* (5), 637–641.
- (46) Lai, C. H.; Chen, K. S.; Wang, H. K. Influence of rice straw burning on the levels of polycyclic aromatic hydrocarbons in agricultural county of Taiwan. *J. Environ. Sci.* **2009**, *21* (9), 1200–1207.
- (47) Timmermann, A.; Oberhuber, J.; Bacher, A.; Esch, M.; Latif, M.; Roeckner, E. Increased El Nino frequency in a climate model forced by future greenhouse warming. **1999**, *Nature* *398*, 694–697.